Direct Measurement of Lattice Dynamics and Optical Phonon Excitation in Semiconductor Nanocrystals Using Femtosecond Stimulated Raman Spectroscopy

Daniel C. Hannah,[1] Kristen E. Brown,[1,2] Ryan M. Young,[1,2] Michael R. Wasielewski,[1,2,3] George C. Schatz,[1,2] Dick T. Co,[1,2] and Richard D. Schaller[1,3,*]

[1]*Department of Chemistry, Northwestern University, Evanston, Illinois 60208-3113, USA*
[2]*Argonne-Northwestern Solar Energy Research (ANSER) Center, Northwestern University, Evanston, Illinois 60208-3113, USA*
[3]*Center for Nanoscale Materials, Argonne National Laboratory, Argonne, Illinois 60439, USA*

(Received 1 March 2013; published 5 September 2013)

We report femtosecond stimulated Raman spectroscopy measurements of lattice dynamics in semiconductor nanocrystals and characterize longitudinal optical (LO) phonon production during confinement-enhanced, ultrafast intraband relaxation. Stimulated Raman signals from unexcited CdSe nanocrystals produce a spectral shape similar to spontaneous Raman signals. Upon photoexcitation, stimulated Raman amplitude decreases owing to experimentally resolved ultrafast phonon generation rates within the lattice. We find a ~600 fs, particle-size-independent depletion time attributed to hole cooling, evidence of LO-to-acoustic down-conversion, and LO phonon mode softening.

DOI: 10.1103/PhysRevLett.111.107401 PACS numbers: 78.67.Bf, 68.65.−k, 73.22.−f, 78.30.Fs

In addition to size-tunable electronic properties [1], quantum-confined semiconductor nanocrystals (NCs) exhibit discrete electronic density of states and carrier energy-level spacings that can significantly exceed the longitudinal optical (LO) phonon energy. Such electronic characteristics led to the prediction of a phonon bottleneck that would substantively slow intraband relaxation [2,3] as only weakly allowed multiphonon processes could facilitate relaxation between widely spaced electronic states. Several studies have shown that, despite this expectation, intraband excitonic relaxation occurs on a sub- to single-picosecond time scale in typical NC compositions [4–8], similar to bulk-phase semiconductors.

Confinement-enhanced electron-to-hole Auger energy transfer has been suggested as the primary means of hot exciton cooling in CdSe NCs where electron excess energy is transferred to holes that then rapidly cool via phonon emission [9]. Experimentally, transient absorption (TA) measurements show faster intraband exciton cooling in smaller particles with larger band gaps [4,5,8], consistent with the proposed mechanism. Since bleach signals in CdSe NCs predominantly arise from excited electrons, these measurements specifically convey NC size-dependent electron cooling rates [10–12]. Recently, Xu *et al.* observed rapid hole cooling times via comparison of TA and femtosecond up-conversion measurements [13]. Similarly, Hendry *et al.* reported ~1 ps electron-hole coupling time based upon transient terahertz measurements [6]. Missing from the literature are direct examinations of lattice dynamics during this process. Such measurements present inherent challenges as the typical subpicosecond carrier relaxation lifetimes and small phonon energies obviate the utility of transient spontaneous Raman spectroscopy [14].

Here, we make use of the recently developed technique of femtosecond stimulated Raman spectroscopy (FSRS), which is known to offer high temporal (~100 fs) and energy (~10 cm^{-1}) resolution [15], to investigate phonon dynamics in photoexcited NCs for the first time. For CdSe NCs, we observe subpicosecond phonon dynamics along with mode softening, and note a lack of size dependence for the initial change in signal levels despite size-dependent electronic intraband relaxation [10–12]. We attribute initial depletion of the FSRS signal to size-independent hot-hole-to-phonon coupling. We also observe a rapid (τ = ~2 ps) recovery of the stimulated Raman signal that is consistent with relaxation of LO phonon populations into other vibrational modes. This rapid phonon down-conversion is followed by a slower recovery of gain amplitude with a time scale and size dependence consistent with phonon outflow from the NC into the surrounding matrix. Diminished gain amplitude at even longer times (~1 ns) is suggestive of persistent LO-phonon generating processes or altered phonon coupling in NCs containing a band-edge exciton, for which the radiative lifetime is on the order of nanoseconds.

We examine hexane suspensions of octadecylamine-capped CdSe NCs with spherical particle shapes, and optical properties as noted in Ref. [16] (see also the Supplemental Material [17]). Figure 1 shows a schematic depicting the FSRS experiment in the context of NC dynamics. The detailed experimental setup has been described previously [18]. Here, we adjust the actinic and Raman pump fluences such that the average number of electron-hole pairs generated per NC is less than 0.2 [12]. This assures that dynamics related to single excitons are observed. Optical Kerr-effect (OKE) cross correlation of the actinic pump and probe pulses in hexane indicates a time resolution of ~170 fs.

Figure 2(a) displays raw FSRS spectra of colloidal CdSe NCs with a 1.5 nm radius. The features observed are

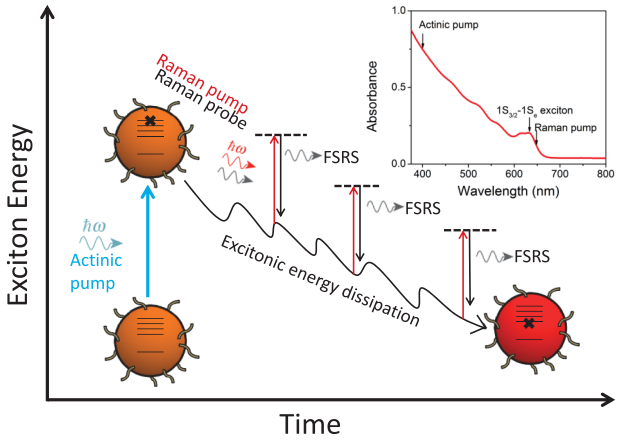

FIG. 1 (color online). An actinic pump photon, having energy greater than the NC energy gap, excites a hot electron-hole pair, denoted by "X". The ladder levels represent exciton (i.e., electron + hole) states. As the system evolves in time, hot carriers cool via various pathways including phonon emission and Auger-like electron-to-hole energy transfer. The Raman pump, which is resonant with electronic transitions in the NC, and probe pulses stimulate Raman transitions at various time delays, generating FSRS signal. Inset: Absorption spectrum of 3.1-nm radius CdSe nanocrystals capped with octadecylamine and suspended in hexane. The actinic pump and Raman pump wavelengths are indicated relative to the $1S_{3/2}$-$1S_e$ exciton transition.

consistent with previous static measurements of resonant Raman scattering in this material [19]. The peak at ± 210 cm^{-1} corresponds to the longitudinal optical (LO) phonon mode of the CdSe lattice and a 2LO phonon Raman peak also appears at ± 410 cm^{-1}. Atypically, the CdSe phonon features exhibit gain at both Stokes and anti-Stokes frequencies (see the Supplemental Material [17]). A low-frequency shoulder on the LO phonon feature, commonly observed in spontaneous Raman spectroscopy [19,20] and attributed to the surface optical (SO) phonon mode [20], is reproducibly observed both here [Fig. 2(a), inset] as well as in static Raman spectra. To analyze each mode, we fit the LO phonon feature using the sum of two Gaussian line shapes as illustrated in the inset of Fig. 2(a). In the dynamics experiments discussed later in this Letter, we note that the LO and SO phonon modes exhibit indistinguishable dynamics, suggestive of a single population exhibiting both phonon features.

Figure 2(b) shows background-subtracted time-resolved spectra for the anti-Stokes 1LO phonon feature at three time delays relative to the 0.5 nJ/cm^2 actinic pump: Both the Stokes (not shown) and anti-Stokes gain amplitudes are depleted by photoexcitation, with partial recovery of the gain signal at longer times. Normalized, background-subtracted 1LO phonon FSRS spectra, presented in Fig. 2(c) for a 2.4 nm radius CdSe NC, prior to (-2 ps) and shortly after (0.1 ps) photoexcitation reveal that the 1LO phonon feature is redshifted by approximately 2 cm^{-1} for both the Stokes and anti-Stokes features. This redshift occurs upon generation of LO phonons by photoexcited NCs. The presence of excitons in NCs leads to a transient renormalization (softening) of the LO phonon frequency. To explain this, we consider the exciton-phonon interaction due to Frolich coupling. The general form of this interaction is shown in Eq. (1) [21],

$$H_{\mathrm{ex-LO}} = \sum_{ij}\sum_{nlm} \gamma^{ij}_{nlm} c_i^{\dagger} c_j (a^{\dagger}_{nlm} + a_{nlm}), \tag{1}$$

where c_i denotes the annihilation operator for the ith exciton state and a_{nlm} is the phonon annihilation operator for the nth phonon mode having angular momentum l. γ^{ij}_{nlm} are the exciton-phonon coupling matrix elements. In the case of strongly confined NCs, excitons couple strongly to LO phonons having $l = 0$ and their coupling can be expressed in terms of sine integrals [22]. The form of the exciton-phonon matrix elements is given by Eq. (2),

$$\gamma^{ij}_{nlm} = -e\sqrt{\frac{\Omega}{\kappa R}}\frac{1}{2n\pi}[\mathrm{Si}((n+i-1)\pi) - \mathrm{Si}((n+i+1)\pi) + \mathrm{Si}((n-i+1)\pi) - \mathrm{Si}((n-i-1)\pi), \tag{2}$$

where Si denotes the sine integral, Ω is the LO phonon frequency, and $\kappa = (\epsilon_0\epsilon_\infty/\epsilon_0 - \epsilon_\infty)$. Once the coupling constants are obtained, the change in the phonon frequency for an excited NC may be calculated using second-order perturbation theory following the procedure described by Zimin *et al.* [21],

$$d\Omega = -\sum_{i\neq 0} \frac{|\gamma^{0i}_n|^2 2(E_i - E_0)}{(E_i - E_0)^2 - \Omega^2}. \tag{3}$$

In Eq. (3), E_i denotes the energy of the ith exciton state. Using Eqs. (2) and (3), we carry out this analysis using CdSe material parameters. For a 2.4-nm radius CdSe NC, we estimate a change in LO phonon frequency upon photoexcitation of -2.6 cm^{-1}, in good agreement with our observation. Figure 2(d) displays the dynamics of the LO phonon peak center for the same sample. Following the initial redshift, the 1LO phonon peak center shifts back towards its original position, but remains slightly redshifted even at time delays of 1 ns, likely owing to a long-lived population of single excitons in photoexcited NCs.

In Fig. 3 we present FSRS dynamics as a function of pump-probe delay for several NC sizes. Figure 3(a) displays the temporal evolution of the 1LO phonon Stokes signal amplitude for the first few picoseconds. Comparison of the instrumental response function (IRF) to the transient phonon signal indicates that the initial dynamical changes in stimulated Raman intensity are well resolved. The early-time FSRS data are dominated by a rapid depletion of the 1LO phonon peak amplitude followed by a slower recovery. Expressions found in the work of Eesley and later McGrane *et al.* [23,24] indicate that stimulated Raman scattering intensity depends exponentially on the inverse of the LO phonon occupation number. FSRS gain intensity can be described by [24]

$$I(\omega_{\mathrm{gain}}, L) = I(\omega_{\mathrm{gain}}, 0) e^{C_{\mathrm{gain}}/(n+1)} \tag{4}$$

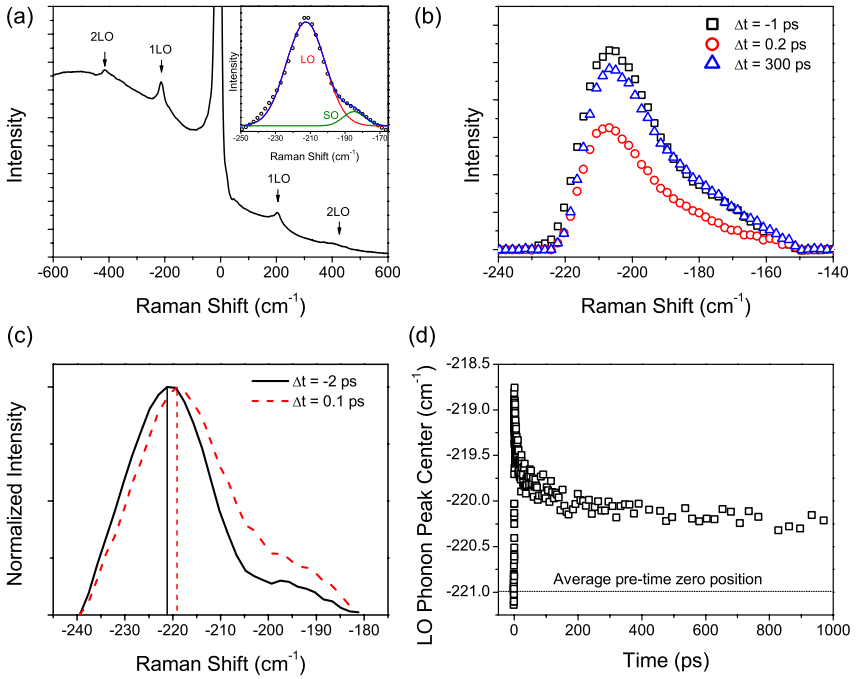

FIG. 2 (color online). (a) Raw ground-state FSRS spectrum for 3.1 nm radius CdSe NCs suspended in hexanes at negative time delay (prior to photoexcitation by the actinic pump). 1LO and 2LO phonon features are indicated. The inset displays a fit of the background-subtracted anti-Stokes peak to the sum of two Gaussian functions. The blue line indicates the overall fit, with the two individual Gaussian functions shown (red and green) and labeled according to their physical origin. In accordance with previous reports, the main peak is assigned to the LO phonon mode, while the low-energy shoulder is assigned to the SO phonon mode. (b) Background-subtracted anti-Stokes phonon peak for 3.1-nm radius CdSe NCs at indicated pump probe time delays. (c) Normalized anti-Stokes phonon band for a 2.4-nm radius CdSe NC at the indicated time delays. The vertical lines serve as a guide to the eye and represent the location of the LO phonon peak center as determined by fits of the phonon band to two Gaussian functions. (d) Dynamics of the LO phonon peak center for a 2.4-nm radius CdSe NC derived from the two-Gaussian fit. The location of the phonon peak center prior to photoexcitation is indicated by the dotted black line.

In Eq. (4), C_{gain} is a collection of terms that depend weakly on temperature; $C_{\text{gain}} = [I(\omega_1)\partial^2\sigma_R/\partial\Omega\partial\Delta\omega] \times (\pi c^4 L\mu_0/8\hbar\omega_{\text{gain}}^3 n_1 n_{\text{gain}}\varepsilon_0)$. Here, L is the sample path length, ω_1 and ω_{gain} are the Raman pump and gain frequency, respectively, n_1 and n_{gain} are the refractive indices of the sample at ω_1 and ω_{gain}, and n is the Bose-Einstein phonon occupation number, given by $n = \exp[(\omega_{\text{LO}}/k_B T) - 1]^{-1}$. Such a dependence taken together with the reduced stimulated Raman gain following excitation strongly suggests that the LO phonon population within the NCs increases following excitation.

Figure 3(b) shows FSRS data for three NC sizes at probe delays up to 1 ns in the main panel, with an intermediate time scale (out to 12 ps) shown in the inset. The data in Fig. 3(b) show a recovery of the depleted LO phonon gain amplitude, indicative of decreased LO phonon occupation number with time. The recovery dynamics (following the Raman gain minimum) exhibit a rapid initial component followed by two slower recovery components. Time constants extracted from triexponential fitting are shown in Table I for three NC sizes [Fig. 3(b)].

The fast Raman gain recovery component (τ_1) exhibits a picosecond time constant that is consistent with the decay of LO phonons into acoustic phonon modes, based upon previous estimates that utilized resonance Raman linewidth analysis [25] [Fig. 3(b), inset]. Recent theoretical studies predict similar time scales for optical phonon relaxation in other materials [26]. This initial rapid recovery exhibits a dependence on NC size, with smaller NCs recovering more rapidly. Similar size dependence is observed for the intermediate component (τ_2). Along with the observed dependence on NC radius, these intermediate time constants ($\tau_2 = \sim$2–20 ps) resemble previously reported time scales for the thermalization of the NC with the surrounding medium [27], but as Ref. [27] measures thermal transport due to *acoustic* phonons, further study will be needed to definitively assign the origin of these dynamics. The slowest component of the recovery (τ_3) exhibits time constants ranging from ~100–230 ps. The time scale of the slower recovery as well as the lack of complete recovery by 1 ns precludes intraband relaxation or biexcitonic Auger recombination, but is consistent with nanosecond time scale recombination (radiative and nonradiative) of excitons and trions [28,29]. The influence of carrier recombination on these processes suggests a contribution to the FSRS signal by photoexcited NCs, a notion supported by the long-lived character of the transient LO-phonon redshift [Fig. 2(c)] [21].

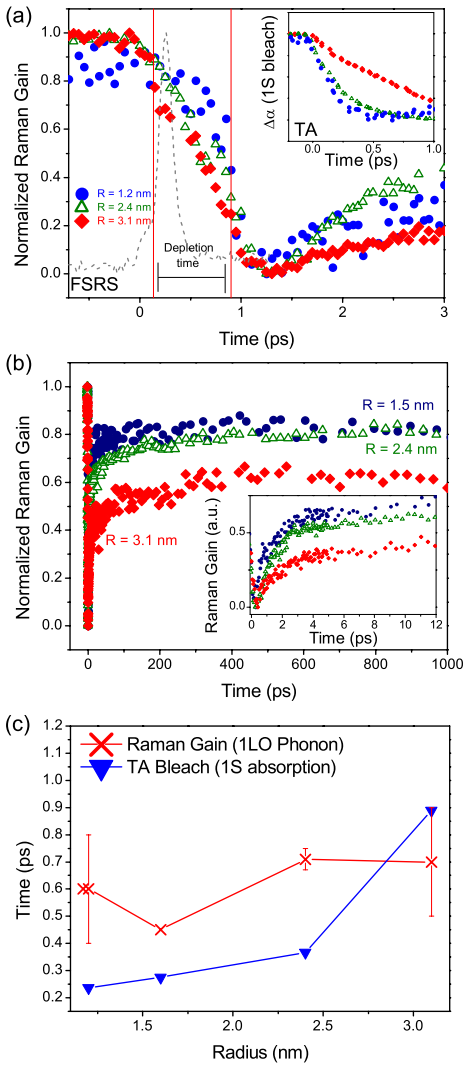

FIG. 3 (color online). (a) Anti-Stokes gain amplitude dynamics at the 1LO phonon frequency for CdSe NCs having radii of 1.2 nm (blue circles), 2.4 nm (green circles), and 3.1 nm (red circles). Data are presented for time delays corresponding to the first few picoseconds before and after the actinic pump arrival ($\Delta t = 0$). The dotted gray line shows the IRF. The vertical red lines indicate the signal depletion time, defined here as the time taken for the signal to drop from 80% to 20% of its initial ($\Delta t < 0$) intensity. The inset displays transient absorption dynamics of the $1S_{3/2}$-$1S_e$ bleach feature for the same set of NCs. (b) Anti-stokes gain amplitude dynamics for 1.5 nm (navy circles), 2.4 nm (green triangles), and 3.1 nm (red diamonds) radius CdSe NCs at time delays up to 1 ns. The inset shows the same dynamics for time delays from 0 to 12 ps. (c) Comparison of measured depletion times for the FSRS 1LO phonon anti-Stokes gain feature (crosses) and the $1S_{3/2}$-$1S_e$ exciton bleach formation time constants (triangles) as a function of NC radius. Error bars represent the standard deviation from multiple measurements, when available.

To further explore the relationship of intraband relaxation to LO phonon generation, we performed a side-by-side comparison with transient absorption measurements under identical experimental conditions by removing the Raman pump beam and instead modulating the actinic pump pulse.

TABLE I. Time constants for Raman gain recovery dynamics extracted from fits to a triexponential function. Errors are derived from the triexponential fits.

Radius (nm)	τ_1 (ps)	τ_2 (ps)	τ_3 (ps)
1.5	0.50 ± 0.07	5.0 ± 0.9	104 ± 34
2.4	1.13 ± 0.05	17 ± 4	229 ± 43
3.1	1.7 ± 0.2	29 ± 19	200 ± 82

The inset of Fig. 3(a) displays early-time TA kinetics for the 1S exciton bleach feature. These data are in close agreement with previous reports [4–7,12] and show the well-known slower intraband relaxation for larger NCs. We observe FSRS depletion dynamics beginning before time zero as identified by TA experiments under identical conditions; we can attribute this pre-time zero signal to an interaction with the picosecond Raman pump pulse the exact nature of which is under investigation. We discuss initial FSRS dynamics in the context of a gain depletion time, which, in this instance, refers to the amount of time needed for the Raman gain to decrease from 80% to 20% of the initial intensity following interaction with the actinic pump. In Fig. 3(c), we compare the 1LO phonon depletion time observed in FSRS [for the feature displayed in Fig. 3(a)] and the 1S bleach formation time from TA [for 1S bleach feature, Fig. 3(a) inset]. While the TA excitonic intraband relaxation depletion times exhibit the expected dependence on NC radius, the FSRS depletion times are relatively independent of size. The rate of LO phonon generation by carrier relaxation in quantum-confined NCs is proportional to the strength of the exciton-LO phonon coupling and the density of states in the valence band, which is only weakly size dependent in the regime

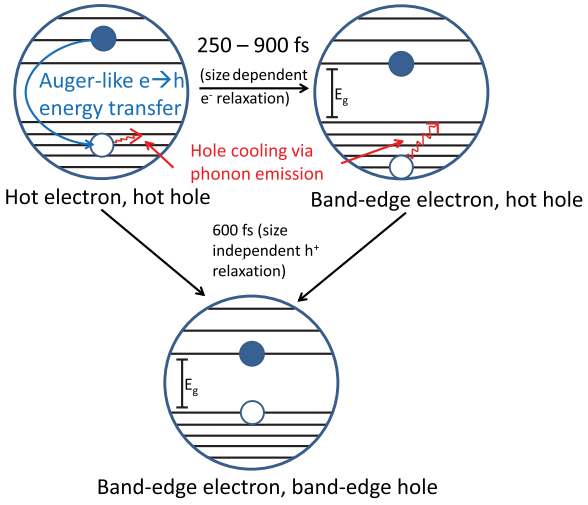

FIG. 4 (color online). Following photoexcitation, Auger energy transfer provides the primary relaxation pathway for the electron. Auger energy transfer rates are dependent on NC size. Conversely, hole cooling is primarily facilitated by LO phonon generation, a process with little or no dependence on NC size for CdSe.

studied here [6,30]. Importantly, the FSRS depletion times measured for the generation of LO phonons are comparable to those observed for the relaxation of the hole to the valence band edge following Auger energy transfer [6,13]. Consistent with this observation, we suggest that hole cooling, rather than electron cooling, principally generates LO phonons, a visual depiction of which is given in Fig. 4 and described here. Estimates of phonon generation in bulk CdSe yield phonon emission times of <1 ps for low excitation densities [31], also consistent with the notion of size-independent phonon generation rates.

In summary, we utilized FSRS to probe the ultrafast dynamics of LO phonons in colloidal CdSe NCs. Changes in stimulated Raman intensity indicate changes in LO population. First, excited charge carriers generate LO phonons during intraband relaxation. Subsequently, LO phonon population is depleted by down-conversion and thermalization processes, which we suggest dominate the NC-size dependent constants τ_1 and τ_2, respectively. To our knowledge, this work constitutes the first direct measurement of LO phonon generation rates in semiconductor NCs. These measurements shed light on the processes by which carrier energy is dissipated in NC lattices, including acoustic phonon down-conversion and thermalization with the surrounding bath. The rate of LO phonon generation is found to be consistent with that for hole cooling, suggesting that holes relax via LO phonon emission subsequent to electron-hole energy transfer. Our work should aid recent theoretical studies that have focused on separate electron and hole relaxation dynamics in the context of vibrational coupling to ligand and phonon modes in the system [32].

This work was performed, in part, at the Center for Nanoscale Materials, a U.S. Department of Energy, Office of Science, Office of Basic Energy Sciences User Facility under Contract No. DE-AC02-06CH11357. D. C. H. acknowledges support from NSF No. DGE-0824162. G. C. S. was supported by Grant No. DE-SC0004752 of the Office of Basic Energy Sciences. D. T. C. and R. M. Y. thank the Camille and Henry Dreyfus Foundation Postdoctoral Program in Environmental Chemistry for support. K. E. B., R. M. Y., D. T. C., and M. R. W. were supported as part of the ANSER Center, an Energy Frontier Research Center funded by the U.S. Department of Energy, Office of Science, Office of Basic Energy Sciences, under Award No. DE-SC0001059.

*schaller@anl.gov
schaller@northwestern.edu

[1] A. P. Alivisatos, Science **271**, 933 (1996).
[2] H. Benisty, C. M. Sotomayor-Torrès, and C. Weisbuch, Phys. Rev. B **44**, 10 945 (1991).
[3] U. Bockelmann and G. Bastard, Phys. Rev. B **42**, 8947 (1990).
[4] V. I. Klimov, D. W. McBranch, C. A. Leatherdale, and M. G. Bawendi, Phys. Rev. B **60**, 13 740 (1999).
[5] P. Guyot-Sionnest, M. Shim, C. Matranga, and M. Hines, Phys. Rev. B **60**, R2181 (1999).
[6] E. Hendry, M. Koeberg, F. Wang, H. Zhang, C. de Mello Donegá, D. Vanmaekelbergh, and M. Bonn, Phys. Rev. Lett. **96**, 057408 (2006).
[7] R. D. Schaller, J. M. Pietryga, S. V. Goupalov, M. A. Petruska, S. A. Ivanov, and V. I. Klimov, Phys. Rev. Lett. **95**, 196401 (2005).
[8] V. I. Klimov and D. W. McBranch, Phys. Rev. Lett. **80**, 4028 (1998).
[9] A. L. Efros, V. A. Kharchenko, and M. Rosen, Solid State Commun. **93**, 281 (1995).
[10] C. Wang, M. Shim, and P. Guyot-Sionnest, Science **291**, 2390 (2001).
[11] I. Robel, M. Kuno, and P. V. Kamat, J. Am. Chem. Soc. **129**, 4136 (2007).
[12] V. I. Klimov, J. Phys. Chem. B **104**, 6112 (2000).
[13] S. Xu, A. A. Mikhailovsky, J. A. Hollingsworth, and V. I. Klimov, Phys. Rev. B **65**, 045319 (2002).
[14] H. Yan, D. Song, K. F. Mak, I. Chatzakis, J. Maultzsch, and T. F. Heinz, Phys. Rev. B **80**, 121403 (2009).
[15] P. Kukura, D. W. McCamant, and R. A. Mathies, Annu. Rev. Phys. Chem. **58**, 461 (2007).
[16] L. Qu and X. Peng, J. Am. Chem. Soc. **124**, 2049 (2002).
[17] See Supplemental Material at http://link.aps.org/supplemental/10.1103/PhysRevLett.111.107401 for sample characterization, Stokes dynamics, and electrostriction calculations.
[18] K. E. Brown, B. S. Veldkamp, D. T. Co, and M. R. Wasielewski, J. Phys. Chem. Lett. **3**, 2362 (2012).
[19] J. J. Shiang, I. M. Craig, and A. P. Alivisatos, Z. Phys. D **26**, 358 (1993).
[20] V. Dzhagan, M. Valakh, N. Mel'nik, O. Rayevska, I. Lokteva, J. Kolny-Olesiak, and D. R. T. Zahn, Int. J. Spectroscopy **2012**, 532385 (2012).
[21] L. Zimin, S. V. Nair, and Y. Masumoto, Phys. Rev. Lett. **80**, 3105 (1998).
[22] A. V. Fedorov and A. V. Baranov, J. Exp. Theor. Phys. **83**, 610 (1996).
[23] G. L. Eesley, J. Quant. Spectrosc. Radiat. Transfer **22**, 507 (1979).
[24] N. C. Dang, C. A. Bolme, D. S. Moore, and S. D. McGrane, Phys. Rev. Lett. **107**, 043001 (2011).
[25] J. J. Shiang, S. H. Risbud, and A. P. Alivisatos, J. Chem. Phys. **98**, 8432 (1993).
[26] L. Tengfei, J. Garg, J. Shiomi, K. Esfarjani, and G. Chen, Europhys. Lett. **101**, 16 001 (2013).
[27] D. C. Hannah, N. J. Dunn, S. Ithurria, D. V. Talapin, L. X. Chen, M. Pelton, G. C. Schatz, and R. D. Schaller, Phys. Rev. Lett. **107**, 177403 (2011).
[28] S. A. Crooker, T. Barrick, J. A. Hollingsworth, and V. I. Klimov, Appl. Phys. Lett. **82**, 2793 (2003).
[29] P. P. Jha and P. Guyot-Sionnest, ACS Nano **3**, 1011 (2009).
[30] D. M. Sagar, R. Cooney, S. Sewall, E. Dias, M. Barsan, I. Butler, and P. Kambhampati, Phys. Rev. B **77**, 235321 (2008).
[31] A. S. Vengurlekar, S. S. Prabhu, S. K. Roy, and J. Shah, Phys. Rev. B **50**, 15 461 (1994).
[32] S. V. Kilina, D. S. Kilin, V. V. Prezhdo, and O. V. Prezhdo, J. Phys. Chem. C **115**, 21 641 (2011).